

A 421 d Activity Cycle in the BeX Recurrent Transient A0538–66 from MACHO monitoring

C. Alcock^{1,2}, R. A. Allsman³, D. R. Alves⁴, T. S. Axelrod⁵, A. C. Becker⁶,
 D. P. Bennett⁷, P. A. Charles⁸, K. H. Cook^{1,2,9}, A. J. Drake¹, K. C. Freeman⁵,
 M. Geha¹⁰, K. Griest^{2,11}, M. J. Lehner¹², S. L. Marshall^{1,9}, K. E. McGowan^{8*},
 D. Minniti^{1,13}, C. A. Nelson¹⁴, B. A. Peterson⁵, P. Popowski¹, M. R. Pratt¹⁵,
 P. J. Quinn¹⁶, C. W. Stubbs^{2,6}, W. Sutherland⁸, A. B. Tomaney⁶, T. Vandehei¹¹,
 D. L. Welch¹⁷

¹Lawrence Livermore National Laboratory, Livermore, CA 94550, USA

²Center for Particle Astrophysics, University of California, Berkeley, CA 94720, USA

³Supercomputing Facility, Australian National University, Canberra, ACT 0200, Australia

⁴Space Telescope Science Institute, Baltimore, MD 21218, USA

⁵Research School of Astronomy and Astrophysics, Canberra, Weston Creek, ACT 2611, Australia

⁶Departments of Astronomy and Physics, University of Washington, Seattle, WA 98195, USA

⁷Department of Physics, University of Notre Dame, Notre Dame, IN 46556, USA

⁸Department of Astrophysics, Nuclear Physics Laboratory, Keble Road, Oxford OX1 3RH

⁹Visiting Astronomer, Cerro Tololo Inter-American Observatory, which is operated by the Association of Universities for Research in Astronomy, Inc., under cooperative agreement with the National Science Foundation

¹⁰Department of Astronomy and Astrophysics, UC Santa Cruz, Santa Cruz, CA 90064

¹¹Department of Physics, University of California, San Diego, La Jolla, CA 92093, USA

¹²Department of Physics, University of Sheffield, Sheffield, S3 7RH

¹³Departamento de Astronomia, P. Universidad Catolica, Casilla 104, Santiago 22, Chile

¹⁴Department of Physics, University of California, Berkeley, CA 94720, USA

¹⁵Center for Space Research, MIT, Cambridge, MA 02139, USA

¹⁶European Southern Observatory, Karl-Schwarzschild Strasse 2, D-85748, Garching, Germany

¹⁷Department of Physics and Astronomy, McMaster University, Hamilton, Ontario, L8S 4M1, Canada

24 October 2018

ABSTRACT

We present a ~ 5 -yr optical light curve of the recurrent Be/X-ray transient A0538–66 obtained as a by-product of the MACHO Project. These data reveal both a long-term modulation at $P = 420.8 \pm 0.8$ d and a short-term modulation at 16.6510 ± 0.0022 d which, within errors, confirms the previously found orbital period. Furthermore, the orbital activity is only seen at certain phases of the 421 d cycle suggesting that the long-term modulation is related to variations in the Be star envelope.

Key words: binaries: close - stars: individual: A0538–66 - X-rays: stars

1 INTRODUCTION

The recurrent X-ray transient A0538–66 was discovered with *Ariel V* when two outbursts, separated by ~ 17 d, were observed (White and Carpenter 1978). Further outbursts were observed with *HEAO-1* which, when the source was active, was found to have a periodicity of 16.668 d (Johnston et al. 1979; Johnston et al. 1980; Skinner et al. 1980; Skinner

1980), the precision of which led to its interpretation as being orbital. Skinner (1981) used archival plates taken over ~ 50 years in order to obtain an improved value of 16.6515 d for this periodicity, based on the recurrence of the outbursts.

A0538–66 has been optically identified with a B star ($V \sim 15$) (Johnston et al. 1980), and an X-ray pulse period of 69 ms indicates that the compact object is a neutron star (Skinner et al. 1982). In quiescence (X-ray ‘off’) the colour, magnitude and radial velocity are consistent with a B2 III-IV star in the LMC (Charles et al. 1983), but during

* email: kem@astro.ox.ac.uk

outburst (which can reach as high as $V \sim 12$; see Densham et al. 1983) it is redder with a spectral type of B8-9 I. During long phases of inactivity (there have been no large X-ray or optical outbursts reported since 1983) there is evidence that a remnant envelope is still present in the system (Smale et al. 1984). A0538-66 has usually been interpreted as a Be-type system which exhibits extreme outbursts as a result of its neutron star companion interacting with the Be star in a highly eccentric orbit (Charles et al. 1983).

Here we exploit the fortuitous location of A0538-66 in a MACHO field and the extended (~ 5 yrs), regular (\sim nightly) monitoring by the MACHO project in order to examine the quiescent variability of this, the most X-ray luminous of all Be X-ray transients.

2 OBSERVATIONS

The MACHO observations were made using the 1.27 m telescope at Mount Stromlo Observatory, Australia. A dichroic beamsplitter and filters provide simultaneous CCD photometry in two passbands, a 'red' band (~ 6300 – 7600 Å) and a 'blue' band (~ 4500 – 6300 Å). The latter filter is a broader version of the Johnson V passband (see Alcock et al. 1995a, 1999 for further details).

The images were reduced with the standard MACHO photometry code SODOPHOT, based on point-spread function fitting and differential photometry relative to bright neighbouring stars. Further details of the instrumental set-up and data processing may be found in Alcock et al. (1995b, 1999), Marshall et al. (1994) and Stubbs et al. (1993).

3 MACHO PROJECT PHOTOMETRY

3.1 Light curve

We show in Fig. 1 the 'blue' and 'red' photometry of A0538-66, the magnitudes of which were transformed to Johnson V and Kron-Cousins R respectively, using the absolute calibration of the MACHO fields. This absolute calibration depends on the colour of the object itself; therefore, at times when there was no red data available a mean colour for the data was used. The data consist of MACHO project observations taken during the period 1993 January 14 to 1998 May 28. There are fewer data points in the R -band because half of one of the four CCD chips in the red focal plane is inoperative. Due to the German telescope mount, the focal plane may be rotated by 0° or 180° relative to the sky (depending on hour angle), hence A0538-66 falls on the dead area in about half the observations. As the V -band light curve has denser sampling than the R -band, only the V -band light curve was used in the rest of the analysis.

3.2 Period analysis and folded light curve

To search for periodicities in the V -band light curve two different frequency domain techniques were employed: (i) we calculated a Lomb-Scargle (LS) periodogram (Lomb 1976; Scargle 1982) on the dataset, to search for sinusoidal modulations [this periodogram is a modified discrete Fourier transform (DFT), with normalizations which are explicitly constructed for the general case of time sampling, including

uneven sampling; see Scargle 1982]; (ii) we constructed a phase dispersion minimisation (PDM) periodogram, which works well even for highly non-sinusoidal light curves (see Stellingwerf 1978).

As a modulation on longer timescales is clearly evident in the light curve the data were searched over the frequency range 0.001 – 0.01 cycle d^{-1} with a resolution of 1×10^{-6} cycle d^{-1} (Figure 2). To search for modulations in the region of the previously quoted 16.6 d period the long term variations were removed. The data were split into 15 sections and each section was detrended separately by subtracting a linear fit. A frequency space of 0.01 – 1.2 cycle d^{-1} was searched with a resolution of 1×10^{-4} cycle d^{-1} (Figure 5).

3.2.1 The 421 d period

In the longer period search a dominant peak is found in the LS periodogram at $P = 420.52$ d (Figure 2). The peak in the LS has a confidence of greater than 99% as determined from a cumulative probability distribution (CDF) appropriate for the data set. By constructing the cumulative probability distribution (CDF) of the random variable $P_X(\omega)$, the power at a given frequency, where X is pure noise (Scargle 1982), we can measure the significance of the peaks in the LS periodogram. In practice the CDF was constructed using a Monte Carlo simulation method. Noise sets with the same sampling as the MACHO data were generated, and the LS periodogram was run upon each one. The peak power occurring in the periodogram due purely to noise was then recorded. This was repeated for ten-thousand noise sets, to produce good statistics. From these values the probability of obtaining a given peak power from pure noise can then be calculated and the CDF derived. In order to test the significance of peaks from a given data set, the generated noise sets should have the same variance. Therefore, each noise set was generated from a random number generator that takes values from a Gaussian distribution with the same variance as the data set. The dip in the PDM periodogram corresponding to the peak in the LS periodogram is broad and highly structured, therefore a centroiding technique was employed to calculate the mode of the dip giving a period of 420.82 d (Figure 2).

The MACHO V -band data were folded on $P = 420.82$ d (Figure 3, top panel), and then binned (Figure 3, middle panel), to examine the form of the modulated variability. Burst points that correspond to the 16.6 d period are evident in the data (see Section 3.2.2), these were removed and the remaining data was bin-folded (Figure 3, bottom panel). To see if the broadness of the peak (FWHM = 6.0×10^{-4} d^{-1}) in the LS periodogram for the longer period search was due to it being quasi-periodic we simulated a truly sinusoidal light curve to be used in period searching. The light curve was produced using a Gaussian random number generator with the same mean and standard deviation as the data plus a sinusoid with a frequency set to the period found. A period search was performed over the frequency range 0.001 – 0.01 cycle d^{-1} with 1×10^{-6} cycle d^{-1} resolution. The resulting LS periodogram is shown as a dashed line in Figure 4. The peak produced from the simulated light curve has a FWHM = 5.5×10^{-4} d^{-1} and is almost as broad as that for the real data which shows that the modulation found is truly periodic.

In order to estimate the uncertainty in the 420.82 d dip in the PDM periodogram we performed a Monte Carlo simulation in which we created artificial light curves with the same mean and standard deviation as the *V*-band data. Phase dispersion minimisation periodograms were constructed and the minimum value found for each artificial dataset using the centroiding technique near the dip of interest was recorded. The results had an average scatter of ± 0.79 d.

3.2.2 The 16.6 d period

The resulting LS periodogram for the short period search has a peak with much greater than 99% confidence at $P = 16.6667$ d, together with two marginally significant peaks around 1 d (Figure 5). To identify the origin of these peaks more simulated datasets were created, which had the same mean and standard deviation as the detrended data. These were produced using a Gaussian random number generator plus a sinusoid with period 16.6667 d. The resulting light curve was searched over a frequency range of 0.01–1.2 cycle d^{-1} with a resolution of 1×10^{-4} cycle d^{-1} . As can be seen from the resulting LS periodogram (Figure 5) the two peaks are 1 d aliases produced due to the sampling of the dataset. Using the centroiding technique again the dip in the PDM periodogram for the short period search was found to correspond to $P = 16.6510$ d (Figure 5).

The detrended *V*-band data were folded on $P = 16.6667$ d and $P = 16.6510$ d using Skinner’s ephemeris (1982). The folded light curves showed that the modulation was highly non-sinusoidal, hence we took the PDM value for the orbital period, and the bin-folded light curve using $P = 16.6510$ d is shown in Figure 6. The error on the period was propagated using the same method as for the long period search producing a value of ± 0.0022 d.

4 DISCUSSION

These extensive MACHO observations have revealed, not only a remarkably stable long-term modulation, but also the presence of the same 16.6 d orbital modulation (in the form of mini-outbursts) that had been seen (on a larger scale) in the 1980’s. But the key additional point is that these mini-outbursts are constrained in 421 d phase to only occur during minima, thereby establishing a physical link between the two. What can this be?

To explain the origins of the long-term variability in A0538–66 it is instructive to consider other systems that show modulations on these timescales. The soft X-ray transient (SXT) 4U 1630–47 is the shortest known recurrent black-hole SXT, with an outburst recurrence interval of ~ 600 –690 d (Jones et al. 1976, Priedhorsky 1986, Kuulkers et al. 1997). The outburst recurrence times vary, as do the intensities at the peak of the outburst and its duration (Kuulkers et al. 1997), this behaviour is also seen in A0538–66 (Skinner et al. 1980). Both sources also undergo transitions between high and low activity on timescales ~ 1 yr (4U 1630–47; Kuulkers et al. 1997, A0538–66; Skinner et al. 1980, Pakull & Parmar 1981), and exhibit inter-outburst activity (4U 1630–47; Parmar et al. 1997, Kuulkers et al. 1997, A0538–66; Densham et al. 1983). Kuulkers et al. (1997)

showed that the outburst recurrence time cannot be related to orbital variations of 4U 1630–47. Due to heavy reddening the optical counterpart has not yet been detected in 4U 1630–47, and so a Be-type secondary cannot be excluded.

Analysis of X-ray observations of another Be/X-ray transient, A0535+26, led to an orbital period of 110.3 d for the source (Finger et al. 1996). Analysis of the long term optical light curve by Clark et al. (1999) showed periodicities at ~ 1400 d, ~ 476 d and ~ 103 d, but no evidence was found for the ~ 110 d presumed orbital period of the neutron star. Clark et al. (1999) could not identify the origin of these quasi-periods, and it was not clear if they were coherent over time.

In normal Be star shell ejection events, which recur on timescales of years, the circumstellar matter lost forms an equatorial disc around the Be star due to its rapid rotation (Slettebak 1987). The Paschen continuum of the equatorial envelope is in emission and thus emits optical light which is redder in *B–V* than that emitted by the early type star. The formation of the disc will either add red light and increase the optical brightness of the system or will mask the early type star and make it appear fainter, depending on the inclination (Corbet et al. 1986, Janot-Pacheco et al. 1987). The photometric behaviour of the Be star in A0538–66 in the *V*, *V–R* diagram (Figure 7) shows a reddening as the source gets fainter. The fading and rising events in A0538–66’s light curve could be due to the formation and depletion of an equatorial disc seen at high inclination.

If this is the case, the fact that the neutron star is believed to be in an eccentric orbit around the Be star could set a limit on the size of the equatorial disc that can form producing the 421 d periodicity. Using this model the mini-outbursts only occur when the disc reaches the upper limit set by the neutron star’s orbit. Although Okazaki (1998) and Negueruela (1999) suggest that the presence of the neutron star in orbit around the Be star will tidally truncate the circumstellar disc of the Be star well within the orbital radius of the neutron star, thus preventing accretion, modelling by Haynes et al. (1980) and Brown and Boyle (1984) shows that matter can escape from the Be star and be spread over a domain in the vicinity of the orbit of the compact star near periastron. Therefore the ‘flat’ part of A0538–66’s light curve is when we are seeing the normal B star without any equatorial disc, hence no outbursts can occur. If this is correct, the previously obtained spectra thought to be taken during ‘quiescence’ were really taken during the extended dips in A0538–66’s light curve. This indicates that the true quiescent magnitude of the system is $\sim V=14.4$, and the quoted quiescent spectral-type must be re-determined. As the colours obtained from the MACHO data are not precise enough we cannot confirm the previously determined spectral classification for A0538–66. A study of archival data of A0538–66, including data taken before 1980, will be presented in a future publication.

Skinner (1981) found the recurrence of the outbursts of A0538–66 to be 16.6515 ± 0.0005 d or 16.6685 ± 0.0005 d. We find the periodicity to be 16.6510 ± 0.0022 d, which within errors confirms the first of Skinner’s previously suggested orbital periods for A0538–66.

5 ACKNOWLEDGEMENTS

KEM acknowledges the support of a PPARC studentship. KEM and PAC thank Malcolm Coe for useful discussions. DM is supported by Fondecyt 1990440. This work was performed under the auspices of the U.S. Department of Energy by University of California Lawrence Livermore National Laboratory under contract No. W-7405-Eng-48.

REFERENCES

- Alcock C., et al., 1995a, *Phys. Rev. Lett.*, 74, 2867
 Alcock C., et al., 1995b, *ApJ*, 445, 133
 Alcock C., et al., 1999, *PASP*, 111, 1539
 Brown J.C., Boyle C.B., 1984, *A&A*, 1984, 141, 369
 Charles P.A., Booth L., Densham R.H., Bath G.T., Thorstensen J.R., Howarth I.D., Willis A.J., Skinner G.K., Olszewski E., 1983, *MNRAS*, 202, 657
 Clark J.S., Lyuty V.M., Zaitseva G.V., Larionov V.M., Larionova L.V., Finger M., Tarasov A.E., Roche P., Coe M.J., 1999, *MNRAS*, 302, 167
 Corbet R.H.D., Smale A.P., Menzies J.W., Branduardi-Raymont G., Charles P.A., Mason K.O., Booth L., 1986, *MNRAS*, 221, 961
 Densham R.H., Charles P.A., Menzies J.W., van der Klis M., van Paradijs J., 1983, *MNRAS*, 205, 1117
 Finger M.H., Wilson R.B., Harmon B.A., 1996, *ApJ*, 459, 259
 Haynes R.F., Lerche I., Wright A.E., 1980, *A&A*, 81, 83
 Janot-Pacheco E., Motch C., Mouchet M., 1987, *A&A*, 177, 91
 Johnston M.D., Bradt H.V., Doxsey R.E., Griffiths R.E., Schwartz D.A., Schwarz J., 1979, *ApJ*, 230, L11
 Johnston M.D., Griffiths R.E., Ward M.J., 1980, *Nature*, 285, 26
 Jones C., Forman W., Tananbaum H., Turner M.J.L., 1976, *ApJ*, 210, L9
 Kuulkers E., Parmar A.N., Kitamoto S., Cominsky L.R., Sood R.K., 1997, *MNRAS*, 291, 81
 Lomb N.R., 1976, *Astrophys. Space Sci.*, 39, 447
 Marshall S., et al., 1994, in MacGillivray H.T., Thomson E.B., Lasker B.M., Reid I.N., Malin D.F., West R.M., Lorenz H., eds., *Proc. IAU Symp. 161, Astronomy from Wide-field Imaging*. Kluwer, Dordrecht, p. 67
 Negueruela I., Roche P., Fabregat J., Coe M.J., 1999, *MNRAS*, 307, 695
 Okazaki A.T., 1998, in Kauer L., Fullerton A.W., eds., *Cyclical Variability in Stellar Winds*, Proceedings of the ESO Workshop held at Garching, Germany, Springer, p. 343
 Pakull M., Parmar A., 1981, *A&A*, 102, L1
 Parmar A.N., Williams O.R., Kuulkers E., Angelini L., White N.E., 1997, *A&A*, 319, 855
 Priedhorsky W.C., 1986, *Ap&SS*, 126, 89
 Scargle J.D. 1982, *ApJ*, 263, 835
 Skinner G.K., Shulman S., Share G., Evans W.D., McNutt D., Meekins J., Smathers H., Wood K., Yentis D., Byram E.T., Chubb T.A., Friedman H., 1980, *ApJ*, 240, 619
 Skinner G.K., 1980, *Nature*, 288, 141
 Skinner G.K., 1981, *Space Sci. Rev.*, 30, 441
 Skinner G.K., Bedford D.K., Elsner R.F., Leaky D., Weisskopf M.C., Grindlay J., 1982, *Nature*, 297, 568
 Slettebak A., 1987, in Slettebak A., Snow T.P., eds., *Proc. IAU Symp. 92, Physics of Be Stars*. Boulder, Colorado, p. 24
 Smale A.P., Charles P.A., Densham R.H., Bath G.T., van Paradijs J., Menzies J.W., Skinner G.K., 1984, *MNRAS*, 210, 855
 Stellingwerf R.F., 1978, *ApJ*, 224, 953
 Stubbs C.W., et al., 1993, in Blouke M., ed., *Proc. SPIE 1900, Charge-coupled Devices and Solid-State Optical Sensors III*. SPIE, Bellingham, p 192
 White N.E., Carpenter G.F., 1978, *MNRAS*, 183, 11

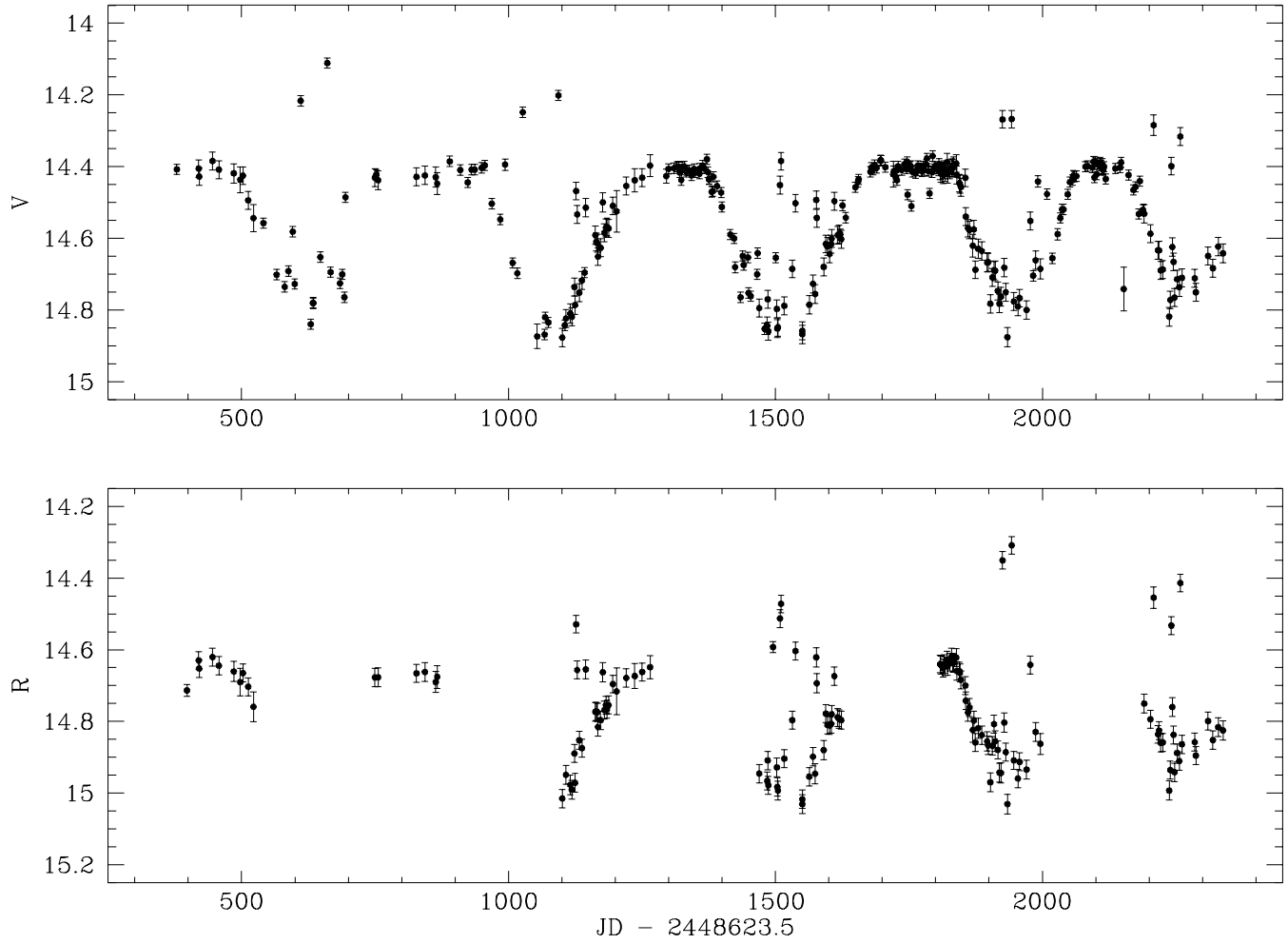


Figure 1. The V - (*top panel*) and R -band (*bottom panel*) light curves of A0538-66 from MACHO project observations. The V and R magnitudes have been calculated using the absolute calibrations of the MACHO fields.

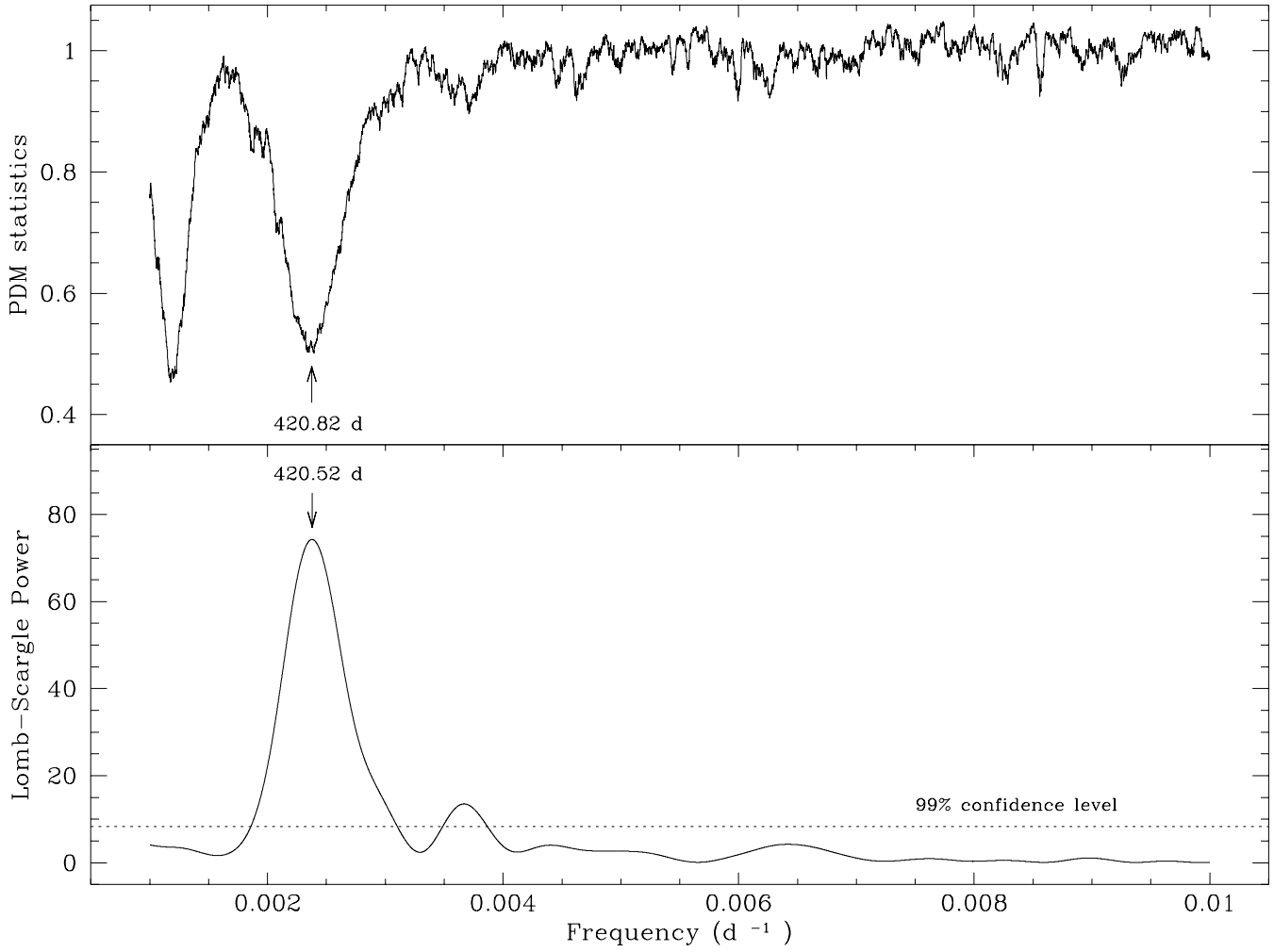


Figure 2. Phase dispersion minimisation periodogram (*top panel*) and Lomb-Scargle periodogram (*bottom panel*) for long period search of V-band data, frequency space 0.001-0.01 cycle d^{-1} and resolution 1×10^{-6} cycle d^{-1} .

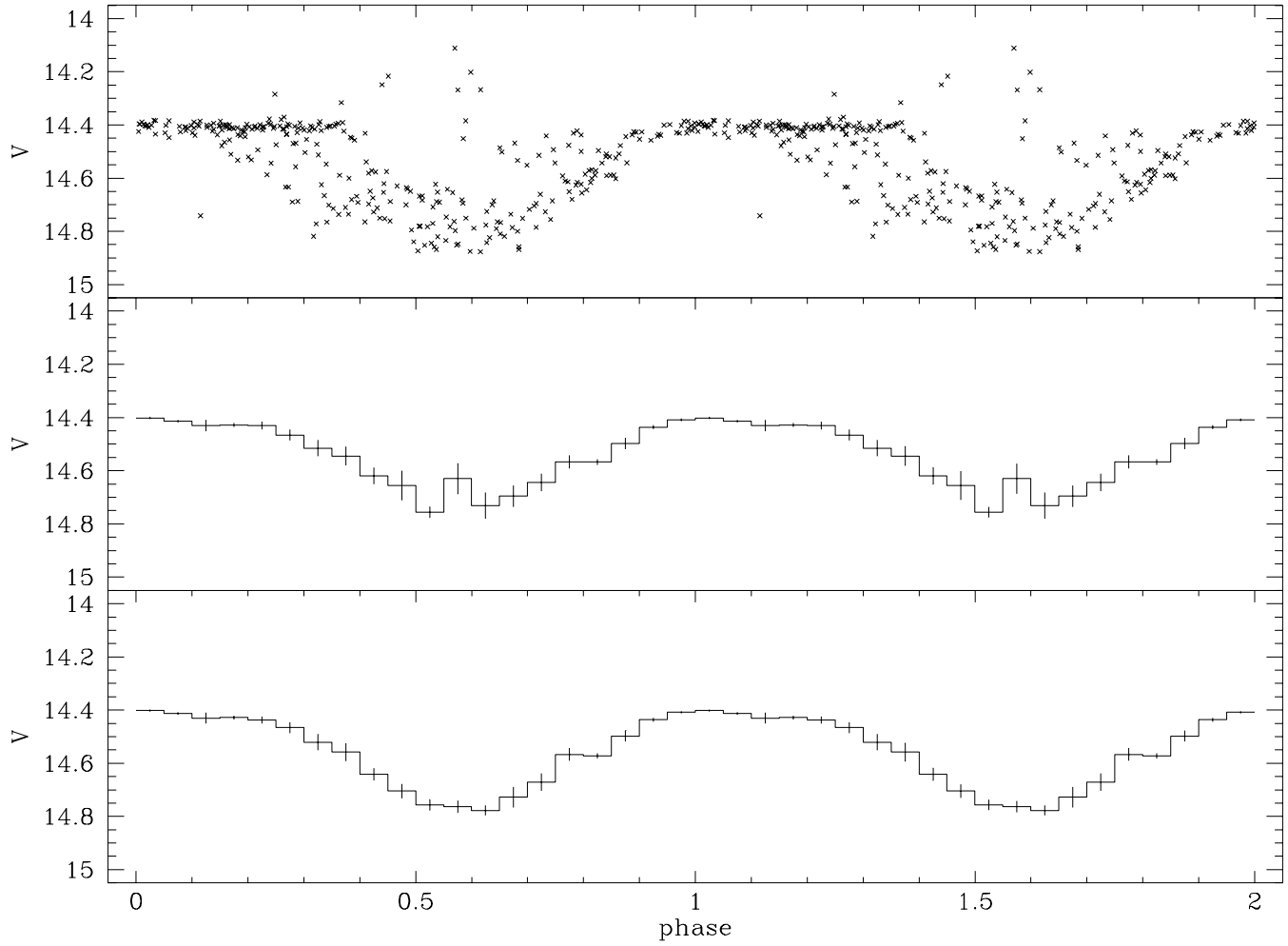


Figure 3. *V*-band data folded on $P = 420.82$ d using $T_o = \text{JD } 2449002.109$ (*top panel*), and in 20 phase bins (*middle panel*). In the *bottom panel* the 16.6510 d burst points have been removed from the data which was then folded into 20 phase bins. Error bars for both binned light curves are the standard errors for the data points in each bin.

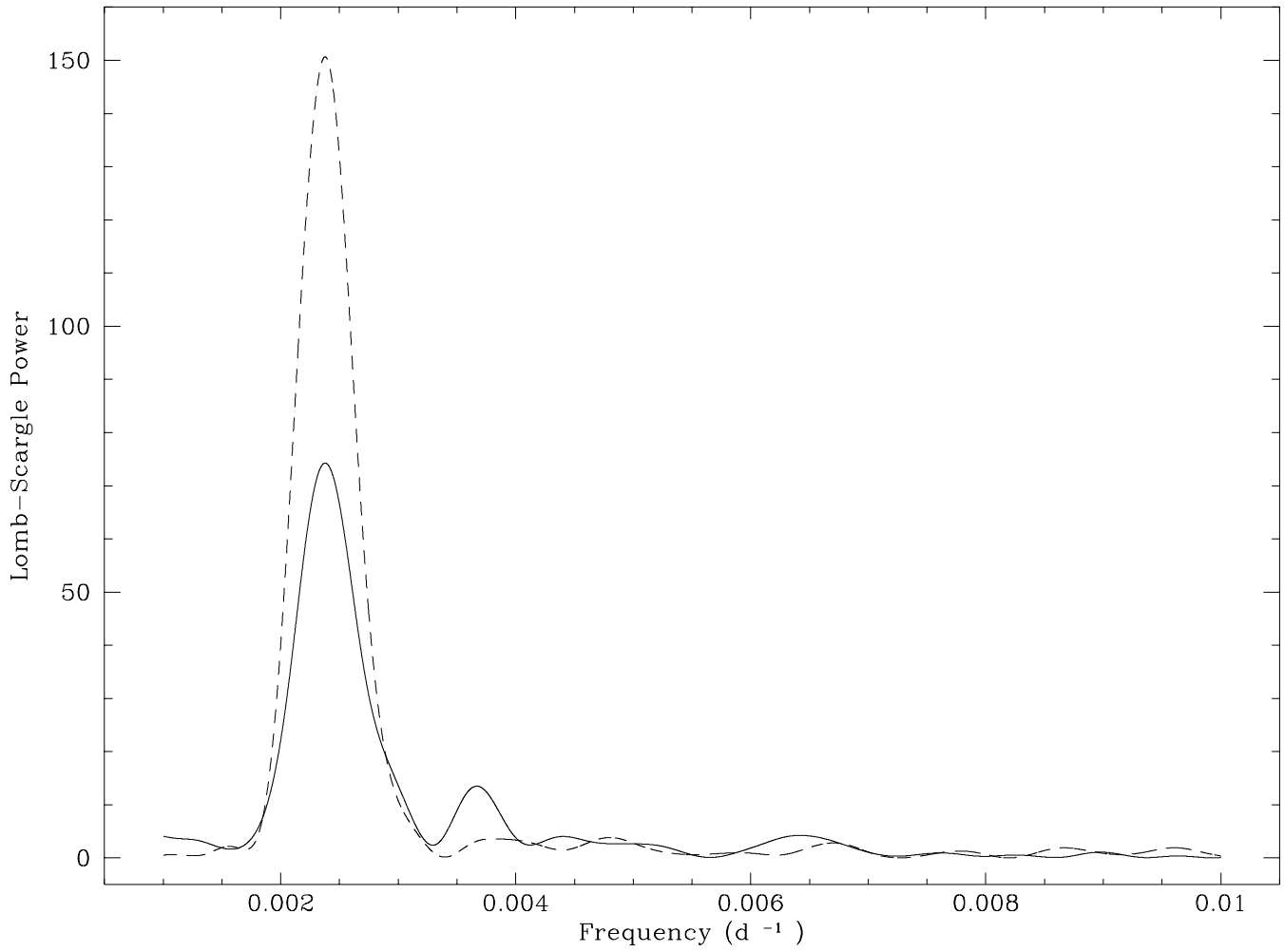


Figure 4. Lomb-Scargle periodogram for long period search of V-band data (solid line) and simulated data (dashed line), frequency space 0.001-0.01 cycle d⁻¹ and resolution 1×10⁻⁶ cycle d⁻¹.

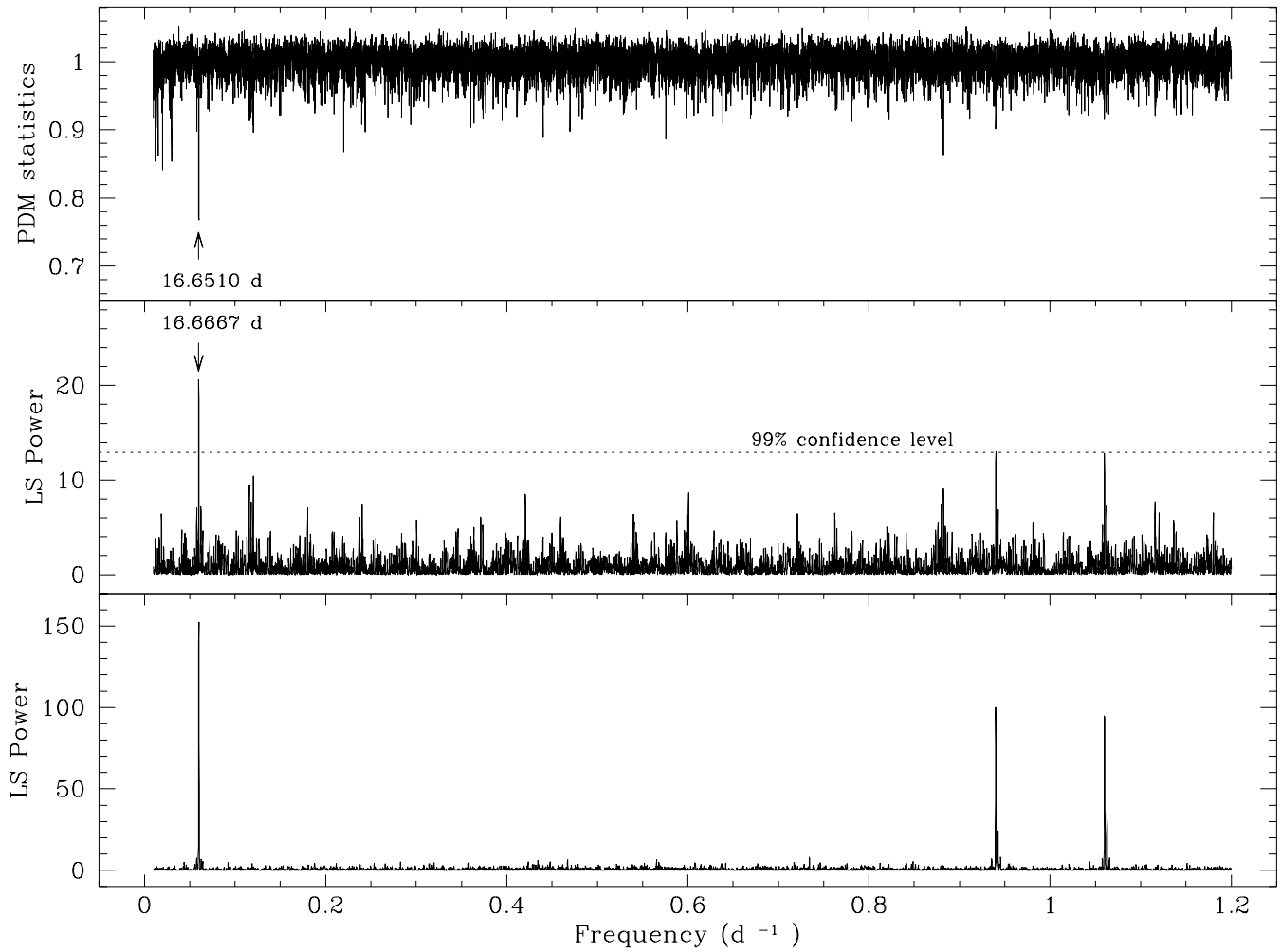


Figure 5. Phase dispersion minimisation periodogram (*top panel*) and Lomb-Scargle periodogram (*middle panel*) for short period search of detrended *V*-band data, frequency space 0.01-1.2 cycle d⁻¹ and resolution 1x10⁻⁴ cycle d⁻¹. *Bottom panel*, Lomb-Scargle periodogram for the simulated light curve which contained a sinusoidal signal of 16.6667 d.

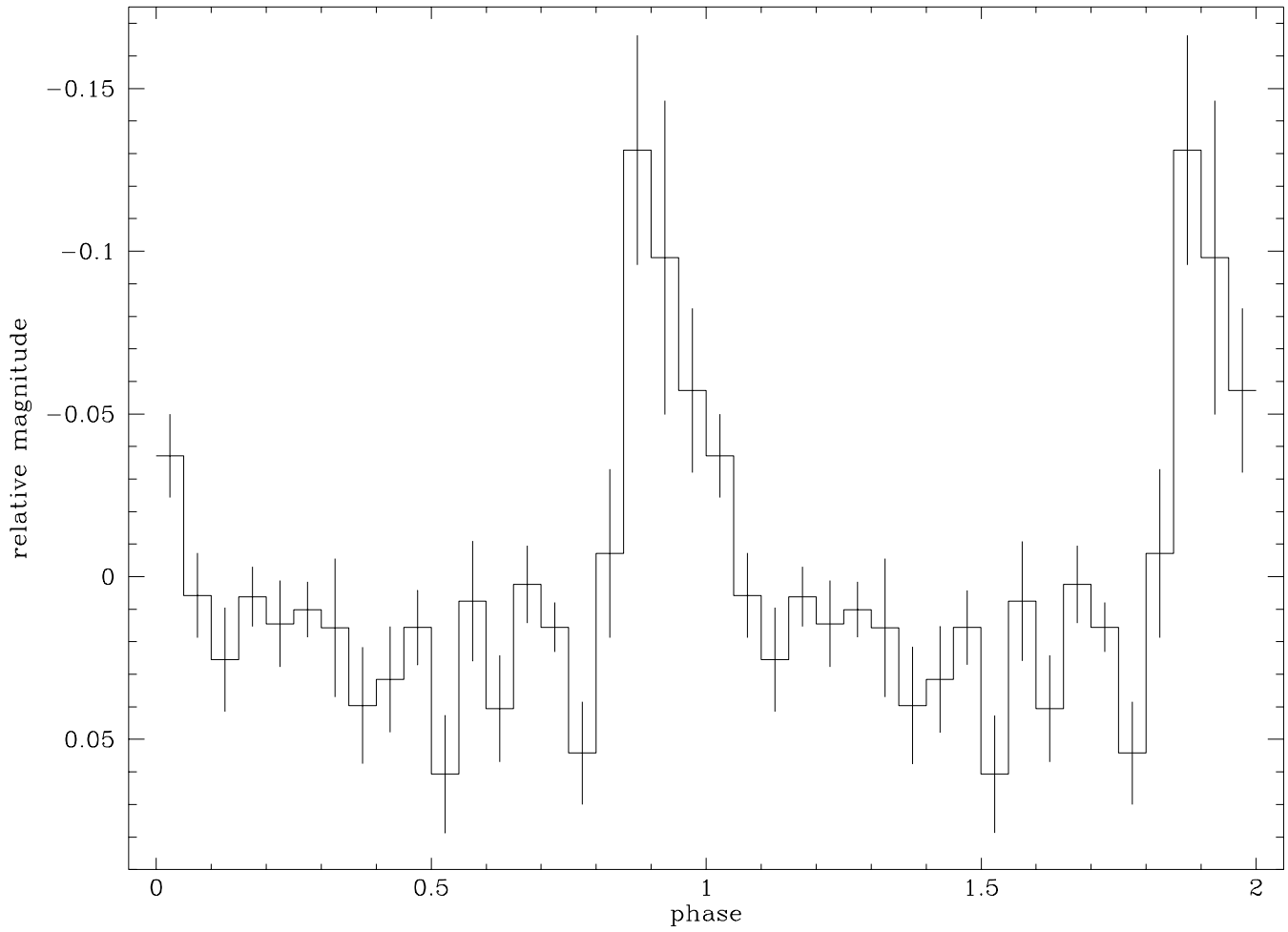


Figure 6. *V*-band data, detrended and folded on $P = 16.6510$ d in 20 phase bins, using $T_0 = \text{MJD } 2443423.96 \pm 0.05$ (Skinner 1981). Error bars for the binned light curve are the standard errors for the data points in each bin.

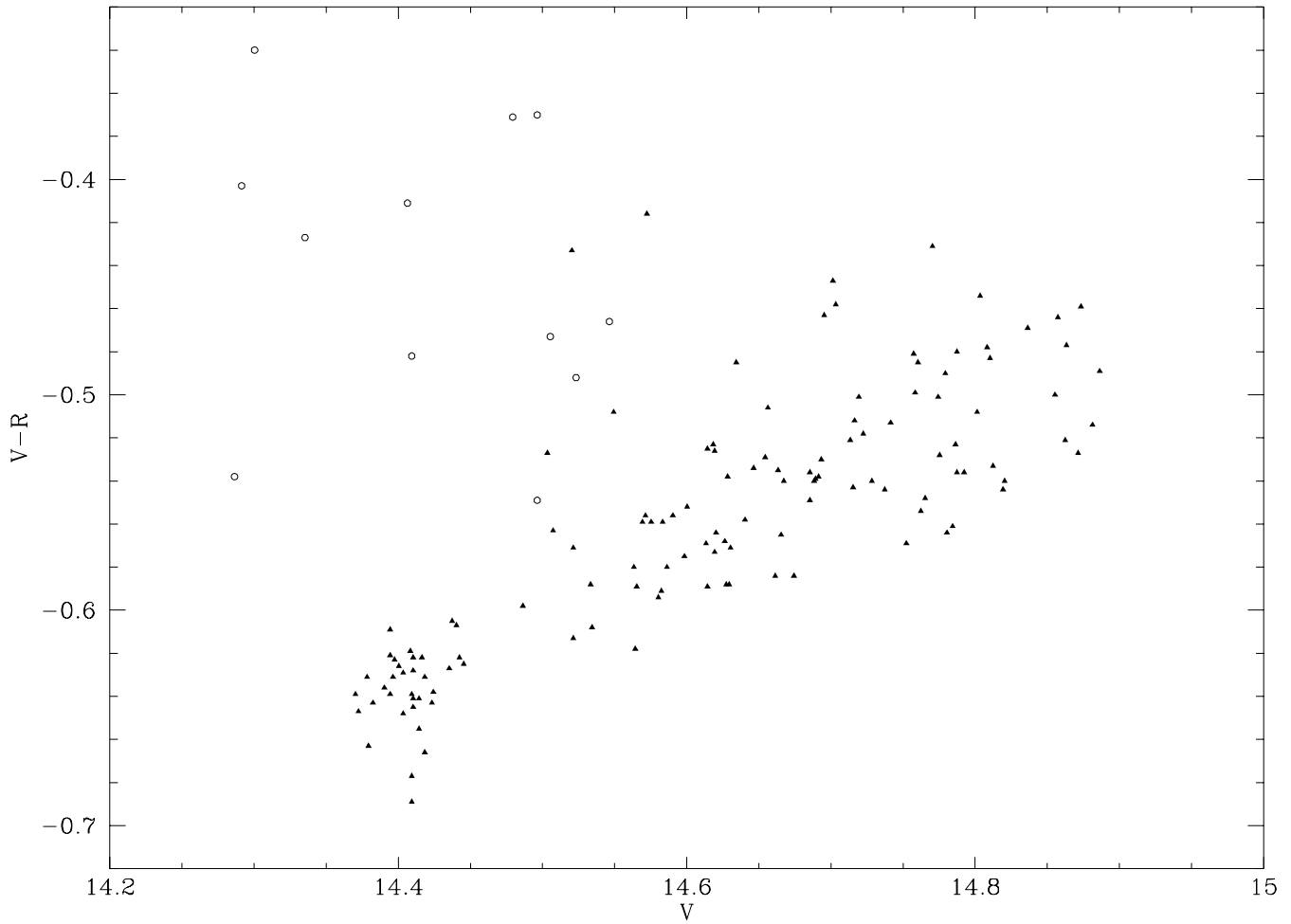


Figure 7. Colour magnitude diagram of A0538-66 showing that the star is redder when fainter which is interpreted in classical Be models as a consequence of the formation of an equatorial envelope seen at high inclination. Open circles correspond to the 16.6510 d burst points, filled triangles to all other data. The $V-R$ values are purely instrumental, whereas the V magnitudes have been calculated using the absolute calibrations of the MACHO fields (see Section 3.1 for details).